A FINITE ELEMENT FORMULATION FOR LARGE ELASTIC-PLASTIC DEFORMATIONS

P. C. M. GORTEMAKER, C. de PATER

Twente University of Technology, Mechanical Engineering Department, Postbox 217, Enschede, The Netherlands

Paper describes numerical and experimental work, which has been done on elastic-plastic problems involving large deformations.

A finite element program has been developed for plane stress and plane strain problems. The frame of reference is a Cartesian updated Lagrangian one. The incremental tangent stiffness method applied, comprises incremental constitutive equations relating the Jaumann increments of Cauchy's "true" stresses to the increments of strains.

The von Mises yield criterion and the rule of normality of the incremental plastic deformation tensor with respect to the yield surface has been used. Isotropic hardening of the material can be taken into account.

The elements are the 3-nodes constant strain and the 4-nodes isoparametric quadrilateral element. Following suggestions made by Nagtegaal et.al. a modified strain increment has been used in the plane strain formulation to prevent difficulties arising from enforced kinematic constraints on the modes of deformation. The incremental tangent stiffness solutions are corrected by an iterative corrective load procedure based upon either the Newton-Raphson or modified Newton-Raphson method. A further refinement which has been built in to correct the stresses is based upon the division of the total strain increment into a number of smaller ones. In this way it is possible to improve the computed resistance produced by the elements by an incremental integration procedure.

The program contains the possibility to prescribe per group of elements their behaviour: linear elastic or elastic-plastic infinitesimal deformations, elastic-plastic finite deformations. The presented theory differs in detail from work published by others.

The purpose of the paper is to show what the effect is of the different options in the computerprogram upon the computed results. In particular, attention will be paid to the effect the inclusion of geometric non-linearity in the computations has upon the distribution of displacements, strains and stresses. To check the mathematical-physical model the results will be compared with data obtained from experimental work.

Paper describes the theoretical basis of a finite element program for elastic-plastic large deformation problems. Some plane stress and plane strain examples are given and results are compared with experimental data.

1. Basic equations.

In the process of deformation of a body a distinction is being made between the following configurations. At time t=0 the body is in its initial undeformed and stress-free state -configuration 0- and the position of its particles are given by its material coordinates a_i with respect to a fixed cartesian coordinate system.

During loading at some time t the configuration 1 is described by the spatial coordinates x_i with respect to the same coordinate system. The assumption is being made that in this configuration all the variables: coordinates x_i, stresses, strains and stress history are known. The stresses and prescribed body and surface forces satisfy the equilibrium conditions and the displacement field is continuous and satisfies prescribed displacements at the boundaries.

Bases of the finite element formulation describing the instantaneous equilibrium and the time derivative of the equilibrium are the virtual power resp. virtual rate of power equations, which must be fulfilled at any time of the deformation process for arbitrary kinematically admissible velocity fields.

The virtual power equation neglecting volume forces in configuration 1 and referred to this configuration is

$$\int_V \sigma_{ij}\, \delta d_{ij}\, dV = R \tag{1}$$

with $$R = \int_S T_i\, \delta v_i\, dS \tag{2}$$

The summation convention with respect to repeated indices is being used.

σ_{ij} are the true Cauchy stresses in the deformed body in configuration 1. δd_{ij} is the virtual rate of deformation tensor and is defined by

$$\delta d_{ij} = \frac{1}{2}\left(\frac{\partial \delta v_i}{\partial x_j} + \frac{\partial \delta v_j}{\partial x_i}\right) \tag{3}$$

in which δv_i are the components of any compatible field of virtual velocities. T_i are the components of the surface forces per unit current surface. dV and dS are volume resp. surface elements in the current configuration 1.

The virtual rate of power equation is derived by taking the material time derivative $[\frac{D}{Dt}(--)$ or $(\dot{--})]$ of eq. (1).

This gives after some manipulation [1,2]

$$\frac{D}{Dt}\left\{\int_V \sigma_{ij}\, \delta d_{ij}\, dV\right\} = \frac{D}{Dt}\left\{\int_V \sigma_{ij} \frac{\partial \delta v_i}{\partial x_j}\, dV\right\} =$$

$$= \int_V \left\{\dot{\sigma}_{ij} - \sigma_{ik}\frac{\partial v_j}{\partial x_k} + \sigma_{ij}\frac{\partial v_k}{\partial x_k}\right\}\frac{\partial \delta v_i}{\partial x_j}\, dV = \dot{R} \tag{4}$$

2. Constitutive relations for elastic-plastic material.

The assumption is made that the material is homogeneous and isotropic and a linear relation between stress rates and strain rates is being adopted. As the elastic strains are small

a linear decomposition of the deformation rate (d_{ij}) into elastic (d_{ij}^e) and plastic parts (d_{ij}^p) is assumed to be valid.

$$d_{ij} = d_{ij}^e + d_{ij}^p \tag{5}$$

The rate of plastic dilatation is zero.

In the constitutive equations frame independent stress rates and deformation rates have to be chosen. This leads to the following relation between the corotational Jaumann rate of Cauchy stresses $(\dot{\sigma}_{ij})^J$ and the rate of elastic deformations

$$(\dot{\sigma}_{ij})^J = C_{ijkl}\, d_{kl}^e \tag{6}$$

The linear elastic material stiffness tensor C_{ijkl} for isotropic material can be written as:

$$C_{ijkl} = \frac{E}{2(1+\nu)} \{\delta_{ik}\,\delta_{jl} + \delta_{il}\,\delta_{jk} + \frac{2\nu}{1-2\nu}\,\delta_{ij}\,\delta_{kl}\} \tag{7}$$

with E being the modulus of elasticity and ν Poisson's ratio, δ_{ij} being Kronecker's delta.

The relation between the Jaumann rate and the material derivative of Cauchy stresses is as follows [3]

$$(\dot{\sigma}_{ij})^J = \dot{\sigma}_{ij} + \omega_{ik}\,\sigma_{kj} - \sigma_{ik}\,\omega_{kj} \tag{8}$$

In this equation the tensor ω_{ij} is the rate of rotation tensor being defined by

$$\omega_{ij} = \frac{1}{2}\left(\frac{\partial v_j}{\partial x_i} - \frac{\partial v_i}{\partial x_j}\right) \tag{9}$$

When we adopt the von Mises yield criterion with isotropic hardening, the equation of the yield surface in stress space can be written as

$$\phi(\sigma_{ij}, \alpha) = (\sigma_{ij} - \frac{1}{3}\,\delta_{ij}\,\sigma_{kk})(\sigma_{ij} - \frac{1}{3}\,\delta_{ij}\,\sigma_{ll}) - 3k_o(k_o + p\alpha) = 0 \tag{10}$$

The term $3k_o^2$ equals $\frac{2}{3}\,\sigma_o{}^2$, σ_o being the yield point in uniaxial tension and p is a positive work hardening parameter. The rate of plastic work dissipation per unit deformed volume is

$$\frac{d\alpha}{dt} = \dot{\alpha} = \sigma_{ij}\, d_{ij}^p \tag{11}$$

and the total specific work dissipation equals

$$\alpha = \int_o^t \sigma_{ij}\, d_{ij}^p\, dt \tag{12}$$

In the case of loading, if plastic deformation takes place the stress point remains on the yield surface, so:

$$\dot{\phi} = \frac{d\phi}{dt} = \frac{\partial \phi}{\partial \sigma_{ij}} \dot{\sigma}_{ij} + \frac{\partial \phi}{\partial \alpha} \dot{\alpha} = 0 \tag{13}$$

As the normality rule is assumed to be valid

$$d\varepsilon_{ij}^{p} = d\lambda \frac{\partial \phi}{\partial \sigma_{ij}} \tag{14}$$

-with $d\lambda$ an infinitesimal scalar multiplier- it can be shown that for materials obeying eq. (10)

$$\frac{\partial \phi}{\partial \sigma_{ij}} \dot{\sigma}_{ij} = \frac{\partial \phi}{\partial \sigma_{ij}} (\dot{\sigma}_{ij})^{J} \tag{15}$$

with the eqs. (5, 6, 10, 11, 13, 14, 15) one can derive that for plastic loading

$$(\dot{\sigma}_{ij})^{J} = (C_{ijkl} - Y_{ijkl})\, d\varepsilon_{kl} \tag{16}$$

in which $Y_{ijkl} = C_{ijpq} \frac{\partial \phi}{\partial \sigma_{pq}} \frac{\partial \phi}{\partial \sigma_{rs}} C_{rskl} \{A + \frac{\partial \phi}{\partial \sigma_{mn}} C_{mntu} \frac{\partial \phi}{\partial \sigma_{tu}}\}^{-1}$ (17)

with $A = 18\, k_o\, (k_o + p\alpha)$

For elastic loading or unloading the constitutive rate relation equals eqs. (6, 7).

3. Derivation of the finite element formulation.

Substitution of eq. (10) in eq. (8) gives with eq. (9) after some manipulation

$$\dot{\sigma}_{ij} = (C_{ijkl} - Y_{ijkl} - C^{*}_{ijkl})\, d\varepsilon_{kl} + \frac{\partial v_i}{\partial x_k} \sigma_{kj} + \frac{\partial v_j}{\partial x_k} \sigma_{ik} \tag{18}$$

with $C^{*}_{ijkl} = \frac{1}{2} (\sigma_{jl}\delta_{ik} + \sigma_{jk}\delta_{il} + \sigma_{il}\delta_{jk} + \sigma_{ik}\delta_{jl})$ (19)

Clearly the tensors C_{ijkl}, C^{*}_{ijkl} and Y_{ijkl} are all symmetric in the indices i and j, k and l, ij and kl. Substitution of eq. (18) in eq. (4) and neglecting the term $\sigma_{ij} \frac{\partial v_k}{\partial x_k} = \sigma_{ij} d\varepsilon_{kk}$ which is small for small elastic strains now leads to the following equation

$$\int_V [(C_{ijkl} - Y_{ijkl} - C^{*}_{ijkl})\, d\varepsilon_{kl} + \sigma_{kj} \frac{\partial v_i}{\partial x_k}] \frac{\partial \delta v_i}{\partial x_j} dV = \dot{R} \tag{20}$$

In this equation the coordinates x_i, stresses σ_{ij}, $\dot{R}$, tensor Y_{ijkl}, volume V are all referred to configuration 1. Discretizing the body into finite elements and the eq. (20) into incremental steps of prescribed loads and displacements leads to a set of linearised equations in increments of the nodal displacements.

In vector-matrix notation this set can be written as

$$(\bar{K} + \bar{G})\, \overrightarrow{\Delta U} = \overrightarrow{\Delta T} + \overrightarrow{\Delta T_C} \tag{21}$$

The vector $\overrightarrow{\Delta U}$ represents the displacement increments of all the nodes. $\bar{K}$ is the tangent stiffness matrix and $\bar{G}$ the initial stress stiffness matrix in configuration 1. $\overrightarrow{\Delta T}$ is the vector of nodal load increments and $\overrightarrow{\Delta T_C}$ the corrective load vector being the

difference between the applied nodal loads and the resistance produced by the elements all in configuration 1.

To maintain or bring the stress state for each integration point on the yield surface at plastic loading a method much alike the one described in [4] has been used. After having solved eq. (21) for $\overrightarrow{\Delta U}$ the stress increments are determined in an integrative way by dividing the displacement increment vector in m equal parts.

$$\overrightarrow{\Delta U}^{*} = \frac{1}{m} \overrightarrow{\Delta U} \tag{22}$$

The stress increments are now determined for each subincrement $\overrightarrow{\Delta U}^{*}$ from eq. (18). All the variables in this equation are now related to the configuration just before applying the pertinent displacement subincrement, the configuration being updated m times for the relevant load increment. The stresses finally computed are the initial stresses for the next load increment. The incremental tangent stiffness solutions may further be corrected by an iterative corrective load procedure.

The computed strains are the Green's strains E_{ij} and the extensions E_i [3].

4. Some numerical results.

The program developed for plane stress and plane strain problems is in use on the DEC-10 computer of the Twente University of Technology. It contains the isoparametric quadrilateral element with a four-point Gausz integration rule and a constant strain triangular element. Following suggestions made in [5] a modified strain increment has been used in the plane strain formulation to prevent difficulties arising from enforced kinematic constraints on the modes of deformation. The program has the possibility to prescribe the behaviour of the elements per element group: linear elastic or elastic-plastic infinitesimal strains, elastic -plastic finite strains.

a) In the first example experimental and computed results are compared. The example is a plate with notch (Fig. 1) The x_1-axis is the axis of symmetry. The material is stainless steel AISI 316. Computations have been made with quadrilateral elements in plane stress. With tensile specimens the average value of the stress across the neck and the "true" stress approximated with the Bridgman formula [6] versus the logarithmic (natural) strain in the neck have been determined for two different overall strain rates. See Fig. 3. The bilinear Cauchy stress-logarithmic plastic strain curve used in the computations is also shown. In Fig. 2 the deformed geometry is shown for a displacement of the loading point of 15.3 mm. In Fig. 4 the extensions E_1 and E_2 at the plane of symmetry are shown for both infinitesimal and finite strain computations. The extension E_2 near the notch is for the finite strain computations considerable larger then for the infinitesimal scheme. In Fig. 5 the normal Cauchy stresses σ_1 and σ_2 at the plane of symmetry are plotted. Figs. 4 and 5 are related to the situation shown in Fig. 2. In Fig. 6 the load-displacement curves for a number of experiments are shown. The curves computed on the basis of the infinitesimal and finite strain schemes are also plotted.

The differences between these curves are small. The computed results appear to be quite sensitive with respect to the chosen stress-strain curve, the discrepancy between computed and experimental results being mainly due to the simplified curve

that has been used.

b) In a second example the problem of growth of voids in an elastic-plastic medium containing a doubly periodic square array of circular cylindrical voids under plane strain conditions and in uniaxial deformation has been studied. Reference is made to [7]. The problem can be reduced to one of a square isolated cell with a hole. From symmetry considerations one can suffice taking a quarter of this cell with appropriate boundary conditions. The finite element mesh of this quadrant is shown in Fig. 7. The cell corresponds to a void concentration of 4.91 percent ($\frac{L_o}{R_o} = 4$). The displacements U_2 in x_2 - direction at the boundary $a_2 = L_o$ have been prescribed. For the sake of comparison of the results the "true" stress-natural strain curve chosen for the computations has been adjusted to the one used in [7]. See Fig. 8. As found by Needleman plastic deformation begins near the void on the x_1-axis and a diagonal band of plastic deformation develops. This region continues to grow until at $\frac{U_2}{L_o} \tilde{\sim} 0.42$ unloading begins. The contraction of the cell $\frac{U_1}{L_o}$ and of the ligament along the x_1-axis between the voids $\frac{U_1^*}{L_o}$ are shown in Fig. 9. In the "early" stage of deformation ($\frac{U_2}{L_o} < 0.40$) the contraction of the cell exceeds the ligament contraction. In the latter stage when unloading spreads across the cell the plastic deformation concentrates in the ligaments between the voids, resulting in a rapid necking down in these regions. In Fig. 9 the quantity $\frac{F}{L_o}$, F being the total load per unit thickness and the average normal true stress σ_a at the boundary $a_2 = L_o$ are plotted also. It appears that the max. load computed occurs at $\frac{U_2}{L_o} \sim 0.10$ and is only 1% lower then the max. value Needleman finds at about $\frac{U_2}{L_o} \sim 0.13$ for this case. In Fig. 9 the relative void volume η is plotted as well. This variable becomes a linear function of $\frac{U_2}{L_o}$ when the cell ceases to contract. The deformed geometry at a strain of $\frac{U_2}{L_o} = 0.53$ is shown in Fig. 10.

When reversing the deformation afterwards the material of the cell deforms plastically and in Fig. 11 the geometry of the cell is plotted at a strain of 10%. The material tends to close the cell along the x_1-axis at a strain of about 5%.

References.

1. J.F. BESSELING, "Non-linear analysis", Proc. World Confress on finite elements methods in structural mechanics, Bournemouth, Oct. 1975.
2. A.W.A. KONTER, Master's thesis, Appl. Mechanics Group, Technical University Delft, April 1977.
3. Y.C. FUNG, Foundations of solid mechanics, Prentice-Hall, 1965.
4. J.R. RICE, D.M. TRACEY, Computational fracture mechanics in Numerical and computer methods in structural mechanics (Ed. by S.J. Fenves et.al.) p. 585, Ac. Press, N.Y., (1973).
5. J.C. NAGTEGAAL et.al., "On numerically accurate finite element solutions in the fully plastic range", Comp. Meth. in appl. mech. and engineering 4, pp. 153-177, 1974.
6. P.W. BRIDGMAN, Studies in large plastic flow and fracture, McGraw-Hill, New York, 1952.
7. A. NEEDLEMAN, "Void growth in an elastic-plastic medium, Trans. ASME Jrnl. Appl. Mech., pp. 964-970, dec. 1972.

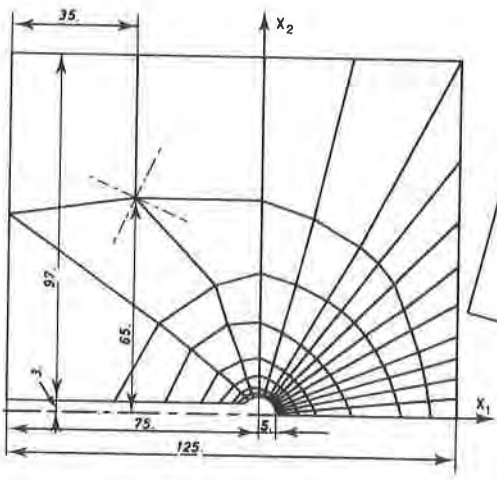

Thickness = 12

Fig. 1. Undeformed geometry of plate
Dimensions in mm.

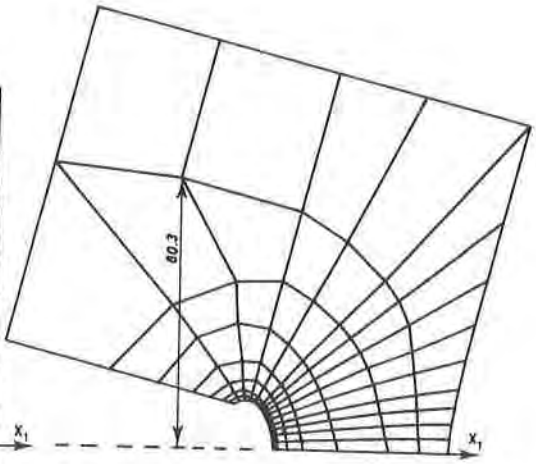

Fig. 2. Deformed geometry computed with finite strain scheme

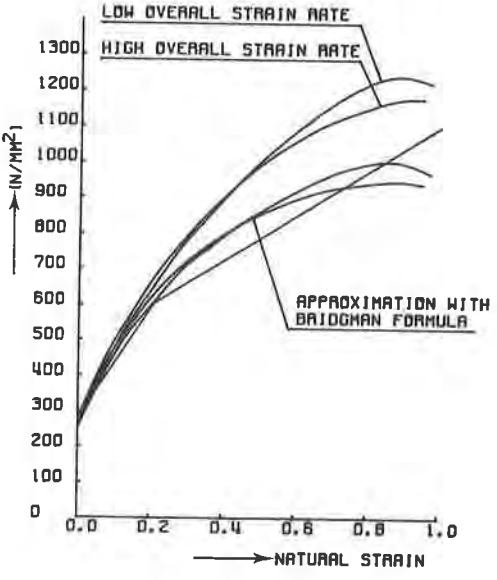

Fig. 3. Stress-strain curves.

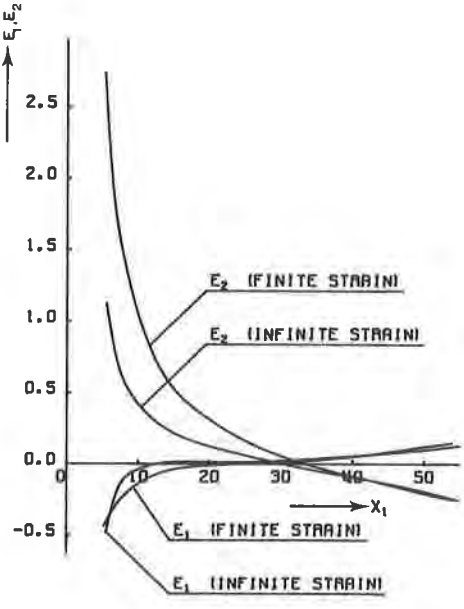

Fig. 4. Extensions at $x_2 = 0$.

ERRATUM

Please correct the figures 4, 5, 6 and 7 as follows :

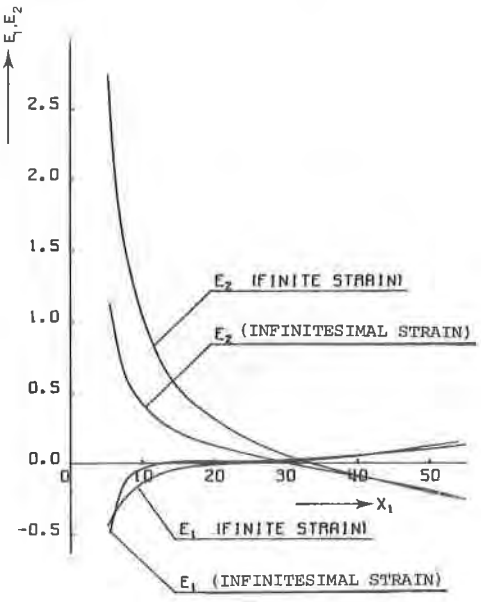

Fig. 4. Extensions at $x_2 = 0$.

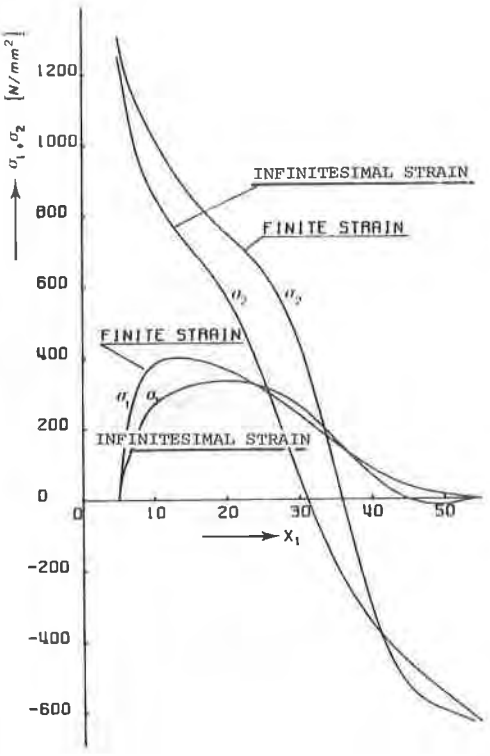

Fig. 5. Stresses at $x_2 = 0$.

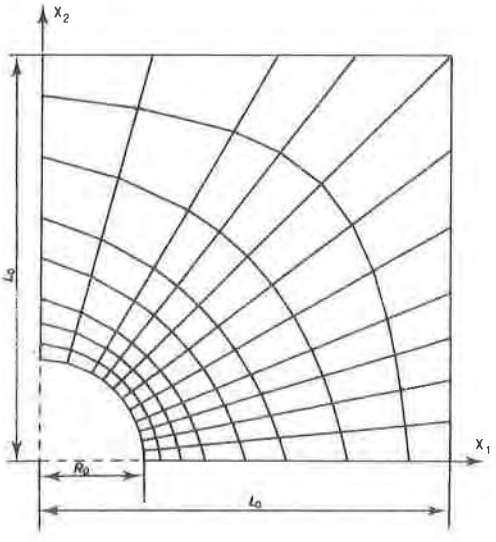

Fig. 7. Undeformed geometry of quadrant of cell.

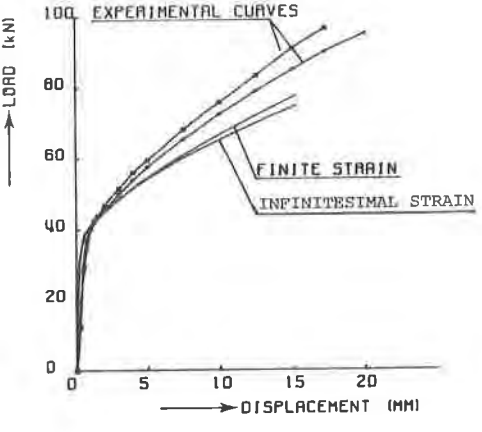

Fig. 6. Load-displacement curves.

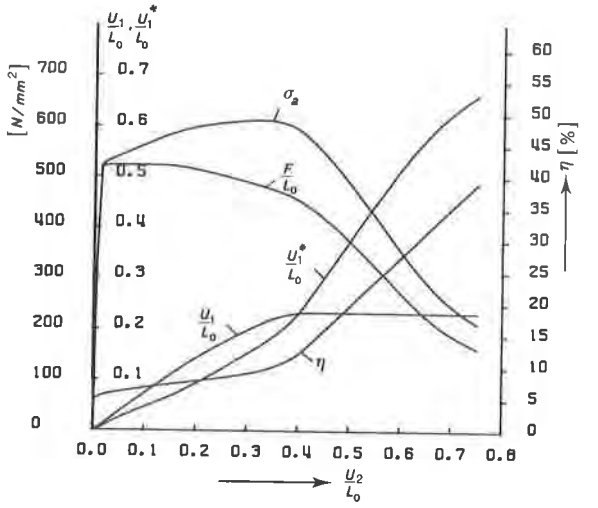

Fig. 9. Average stresses at $a_2 = L_0$, contractions, void volume.

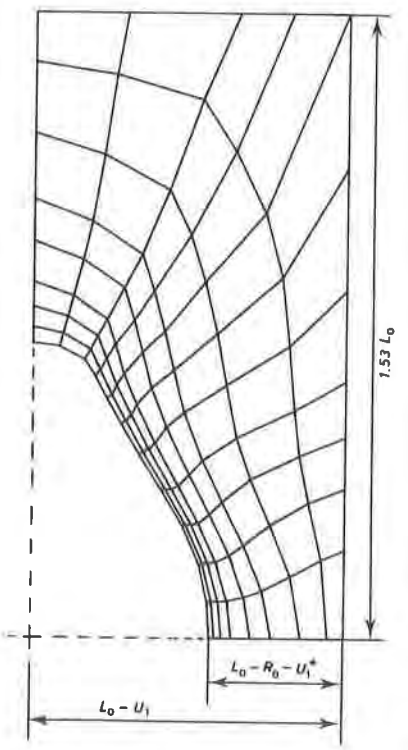

Fig. 10. Deformed geometry of quadrant at $U_2/L_0 = 0.53$.

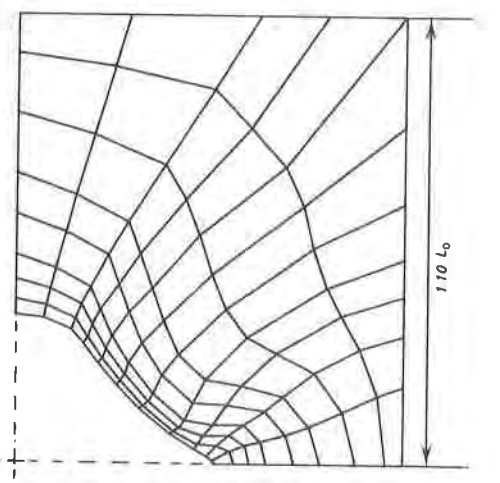

Fig. 11. Deformed geometry at $U_2/L_0 = 0.10$ after load reversal from $U_2/L_0 = 0.53$